© 2018. Published by The Company of Biologists Ltd | Development (2018) 145, dev169201. doi:10.1242/dev.169201

RESEARCH ARTICLE

Independent yet overlapping pathways ensure the robustness and responsiveness of trans-Golgi network functions in *Arabidopsis*

Raksha Ravikumar[1,*], Nils Kalbfuß[1,*], Delphine Gendre[2], Alexander Steiner[1], Melina Altmann[3], Stefan Altmann[3], Katarzyna Rybak[1], Holger Edelmann[1], Friederike Stephan[1], Marko Lampe[4], Eva Facher[5], Gerhard Wanner[6], Pascal Falter-Braun[3,7], Rishikesh P. Bhalerao[2] and Farhah F. Assaad[1,‡]

ABSTRACT

The trans-Golgi-network (TGN) has essential housekeeping functions in secretion, endocytosis and protein sorting, but also more specialized functions in plant development. How the robustness of basal TGN function is ensured while specialized functions are differentially regulated is poorly understood. Here, we investigate two key regulators of TGN structure and function, ECHIDNA and the Transport Protein Particle II (TRAPPII) tethering complex. An analysis of physical, network and genetic interactions suggests that two network communities are implicated in TGN function and that ECHIDNA and TRAPPII belong to distinct yet overlapping pathways. Whereas ECHIDNA and TRAPPII colocalized at the TGN in interphase cells, their localization diverged in dividing cells. Moreover, ECHIDNA and TRAPPII localization patterns were mutually independent. TGN structure, endocytosis and sorting decisions were differentially impacted in *echidna* and *trappii* mutants. Our analyses point to a partitioning of specialized TGN functions, with ECHIDNA being required for cell elongation and TRAPPII for cytokinesis. Two independent pathways able to compensate for each other might contribute to the robustness of TGN housekeeping functions and to the responsiveness and fine tuning of its specialized functions.

KEY WORDS: TGN, ECHIDNA, TRAPPII, Network interactions, Sorting, Cytokinesis

INTRODUCTION

The trans-Golgi network, or TGN, is emerging as a major hub for the flow and sorting of information from and to the cell surface (Gendre et al., 2015; Rosquete et al., 2018; Uemura and Nakano, 2013). At the TGN, macromolecules are sorted into different populations of vesicles destined for the cell surface or for the vacuole. As it is the first point of entry for information from the cell surface, the TGN is also referred to as an early endosome in plants (Dettmer et al., 2006). The TGN plays three essential functions in membrane trafficking: exocytosis, endocytosis and protein sorting (Rosquete et al., 2018). In addition, it plays important roles in more specialized cellular processes, such as the establishment of polarity, cell differentiation, anisotropic growth and cytokinesis (Gendre et al., 2015; Ravikumar et al., 2017). Thus, sorting decisions at the TGN likely give rise to differential growth decisions. In spite of the central importance of the TGN in post-Golgi traffic and endosomal trafficking, several key questions as to TGN structure and function remain unanswered. In particular, TGN structural organization into overlapping but distinct sub-compartments remains poorly understood. Furthermore, it is unclear how environmental or developmental cues regulate the cargo composition and sorting of TGN vesicles. Nor is it clear how specialized TGN functions are differentially regulated by different cues.

Electron tomography has shown that the plant TGN arises from the Golgi by a process of cisternal peeling, which leads to the separation of the TGN cisternae from the Golgi stack and to the formation of independent compartments (Kang et al., 2011). As they mature, TGN cisternae are released from the stack at the trans-Golgi and produce secretory and clathrin-coated vesicles. At the end of their life cycle, mature TGN compartments fragment into vesicles (Staehelin and Kang, 2008). The ratio of secretory to clathrin-coated vesicles is highly variable between individual TGN cisternae, even within a single cell (Kang et al., 2011). Thus, electron tomography highlights the plasticity of the plant TGN (Staehelin and Kang, 2008), which likely underlies a reprograming of the composition and destination of TGN vesicles in response to environmental or developmental cues.

Proteomic approaches have been deployed to gain mechanistic insight into TGN function. Surprisingly, only 30 proteins were identified as being TGN resident; these are required for membrane traffic, ion or metal transport, water homeostasis, proteolysis, protein folding, carbon and lipid metabolism, cell wall biosynthesis, senescence or cell death, development and biotic interactions (Groen et al., 2014). In the transmembrane transport or membrane traffic categories are several proteins involved in vacuolar targeting: a Rab GTPase interacting protein (YIP1), and two SNAREs (SYP61 and VAMP727) required for vesicle docking and fusion (Groen et al., 2014). There are also a number of unknown proteins, such as ECHIDNA, which forms a complex with YIP proteins (Gendre et al., 2013) and which is a component of SYP61 vesicles (Drakakaki et al., 2012).

ECHIDNA was originally identified by virtue of its transcriptional upregulation in elongating cells in both *Arabidopsis thaliana* (*Arabidopsis*) and hybrid aspen; consistently, *echidna* mutants are impaired in cell elongation (Gendre et al., 2011). In addition,

[1]Plant Science Department, Botany, Technische Universität München, 85354 Freising, Germany. [2]Umeå Plant Science Centre, Forest Genetics and Plant Physiology, Swedish University of Agricultural Sciences, S-901 83 Umeå, Sweden. [3]Institute of Network Biology (INET), Helmholtz Zentrum München, Deutsches Forschungszentrum für Gesundheit und Umwelt (GmbH), 85764 Neuherberg, Germany. [4]Advanced Light Microscopy Facility, EMBL Heidelberg, 69117 Heidelberg, Germany. [5]Systematic Botany and Mycology, Faculty of Biology, Dept. I Ludwig-Maximilians-Universität, 80638 Munich, Germany. [6]Faculty of Biology, Dept. I, Ludwig-Maximillians Universität, 82152 Planegg-Martinsried, Germany. [7]Faculty of Biology, Microbe-Host-Interactions, Ludwig-Maximilians-Universität (LMU) München, 82152 Planegg-Martinsried, Germany.
*These authors contributed equally to this work

‡Author for correspondence (farhah@wzw.tum.de)

D.G., 0000-0001-9230-0585; K.R., 0000-0003-3595-0818; G.W., 0000-0002-5996-5902; P.F., 0000-0003-2012-6746; R.P.B., 0000-0003-4384-7036; F.F.A., 0000-0002-8683-9039

Received 26 June 2018; Accepted 2 October 2018

Development (2018) 145, dev169201. doi:10.1242/dev.169201

echidna mutants have defects in hook formation and in pollen formation, release and fertilization (Boutté et al., 2013; Fan et al., 2014; Gendre et al., 2013). Electron tomography of *echidna* mutants, together with a genetic analysis of protein and polysaccharide secretion, yielded striking phenotypes, which suggest that ECHIDNA is primarily required for the genesis of secretory vesicles (Boutté et al., 2013; Gendre et al., 2013; McFarlane et al., 2013).

A complex with functions that overlap with those of ECHIDNA at the plant TGN is the Transport Protein Particle II (TRAPPII) tethering complex. Both ECHIDNA and TRAPPII are required for exocytosis and protein sorting but neither have been implicated in endocytosis (Boutté et al., 2013; Gendre et al., 2011, 2013; McFarlane et al., 2013; Qi et al., 2011; Rybak et al., 2014). TRAPPII is an octomeric complex consisting of four core-TRAPP subunits: an adaptor, a subunit required for complex formation and two large TRAPPII-specific subunits – AtTRS120/VAN4 and AtTRS130/CLUB (Ravikumar et al., 2017). AtTRS120 and AtTRS130/CLUB were identified in forward and reverse genetic screens for cytokinesis-defective mutants in *Arabidopsis*; null alleles are seedling lethal with canonical cytokinesis defects such as multinucleate cells with incomplete cross walls (Jaber et al., 2010; Thellmann et al., 2010). Plant cytokinesis takes place in a TGN-derived compartment referred to as the cell plate (Chow et al., 2008). The TRAPPII complex is required for cell plate biogenesis and localizes to the cell plate throughout cytokinesis (Ravikumar et al., 2017; Rybak et al., 2014). Cell plate biogenesis, which is regulated by cell cycle cues, is a good model for specialized TGN functions in plants. It is not clear whether the cell plate is derived from a subpopulation of TGN sub-compartments responsive to cell cycle cues, or whether cytokinetic vesicles arise from generic TGN subdomains.

ECHIDNA and the two TRAPPII-specific loci (AtTRS120 and AtTRS130/CLUB) are encoded by single copy genes in *Arabidopsis*. The surprising observation that null mutants survive until or past the seedling stage points to the robust nature of essential TGN functions and to the possible existence of functional redundancy or backup mechanisms. Whether ECHIDNA and TRAPPII act in concert or independently of each other to orchestrate the diverse functions of the plant TGN is unclear. Similarly, little is known about how developmental and/or cell cycle cues are integrated into sorting decisions. ECHIDNA and TRAPPII have thus far been studied largely with different markers in different tissues or at different time points, with an emphasis on interphase cells for ECHIDNA and on cytokinetic cells for TRAPPII. Thus, functional comparisons are hard to draw. In this study, we analyze colocalization, secretion, endocytosis and sorting, applying high- and/or super-resolution microscopy. We explore functional and network interactions and the interdependence of the proteins on each other. Our findings highlight the differences between ECHIDNA and TRAPPII, especially in dividing cells, as well as the dynamic nature of TGN structure and function in *Arabidopsis*.

RESULTS

ECHIDNA and TRAPPII colocalize at the TGN but not at the cell plate

As ECHIDNA and TRAPPII are both associated with the TGN, we first tested whether we could spatially resolve them using confocal laser scanning microscopy (CLSM) using antibody stains against native ECHIDNA or against GFP to detect TGN-related markers or TRAPPII subunits in root tips (Table S1; Fig. 1A-C). ARA7-GFP, which is on a gradient between the TGN and late endosome, was used as a control; VHA-a1-GFP, which is exclusively detected on TGN cisternae, was used as a bona fide TGN marker (Dettmer et al., 2006; Gendre et al., 2015). The highest degree of spatial association was observed in interphase cells between ECHIDNA and the TRAPPII subunit TRS120-GFP (Rybak et al., 2014), with a Pearson's correlation coefficient r=0.88 (Fig. 1C,D), which is a significantly (P=0.0003) higher degree of colocalization than observed between ECHIDNA and VHAa1-GFP (r=0.81; Fig. 1B,D). We then analyzed the localization of the proteins using stimulated emission depletion (STED) super-resolution microscopy, with a spatial resolution of 50-70 nm. As expected, the higher resolution provided greater detail but did not change the overall picture: ECHIDNA and ARA7-GFP labelled structures were distinct but in close proximity to each other; ECHIDNA and VHAa1-GFP resided on partially overlapping structures, whereas ECHIDNA and TRS120-GFP still appeared to colocalize almost completely to the same structures in interphase cells (Fig. S1). In mitotic cells, ECHIDNA also strongly colocalized with TRS120-GFP at the TGN, as assessed with STED and antibody stains (PCC=0.91; Fig. 1D). To better monitor cell plate localization throughout cytokinesis, we carried out live imaging of dividing cells. This revealed a dynamic change in the localization pattern of ECHIDNA-YFP (Gendre et al., 2011) and TRS120-mCherry (Rybak et al., 2014) with TRS120-mCherry labeling the cell plate and cytosol, whereas ECHIDNA-YFP did not, even though it appeared in the vicinity of the cell plate (Fig. 1E). In conclusion, ECHIDNA and TRAPPII colocalized at the TGN in both interphase and mitotic cells but their localization patterns diverged at the cell plate.

TGN structure is differentially impacted by *echidna* and *trapii* mutations

TGN structure has been shown to be affected in both *echidna* and *trappii* mutants (Boutté et al., 2013; Gendre et al., 2011; McFarlane et al., 2013; Qi et al., 2011). We confirmed a previous result (Qi et al., 2011) that TGN structures are undetectable by transmission electron microscopy (TEM) in a null allele of the *TRAPPII* locus *AtTRS130/CLUB* (*club-2* root tips; Table S2; Fig. 2B, compare with Fig. 2A). In contrast, we did identify canonical TGN structures for a null allele of the second *TRAPPII*-specific locus, *AtTRS120* (*trs120-4* root tips; Table S2; Fig. 2C). This finding was surprising as the two TRAPPII-specific loci have hitherto been described as being interchangeable (Qi et al., 2011). We followed through by imaging TGN markers in *echidna* and *trappii* interphase root tip cells using high resolution CLSM (Fig. 2D-I). In *club-2* mutants, there was a decrease in the average size of VHAa1-GFP-positive compartments when compared with the wild type (Fig. 2E,F; P=0.0001). In contrast to *club-2*, VHAa1-GFP-positive compartments formed aggregates in *trs120-4* mutants (Fig. 2E,F). For SYP61-CFP (Robert et al., 2008), a SNARE highly colocalizing with VHA-a1, *echidna* and *trappii* exhibited opposite trends: particle or aggregate size was increased in *echidna* (Fig. 2H,I; P<0.05 for *echidna*) and decreased in *trappii* (Fig. 2H,I; P=4e^{-11} for *club-2* and 4e^{-05} for *trs120-4*). Taken together, our findings indicate that *echidna* and *trappii* mutants have a measurable but different impact on TGN structure. Surprisingly, both TEM and high-resolution CLSM showed that TGN structure was more severely impacted in *club-2* than in *trs120-4* mutants.

echidna and *trappii* mutants have different impacts on endocytosis, cell elongation and cytokinesis

Both ECHIDNA and TRAPPII have been implicated in exocytosis but neither was thought to be required for endocytosis (Gendre et al.,

Development (2018) 145, dev169201. doi:10.1242/dev.169201

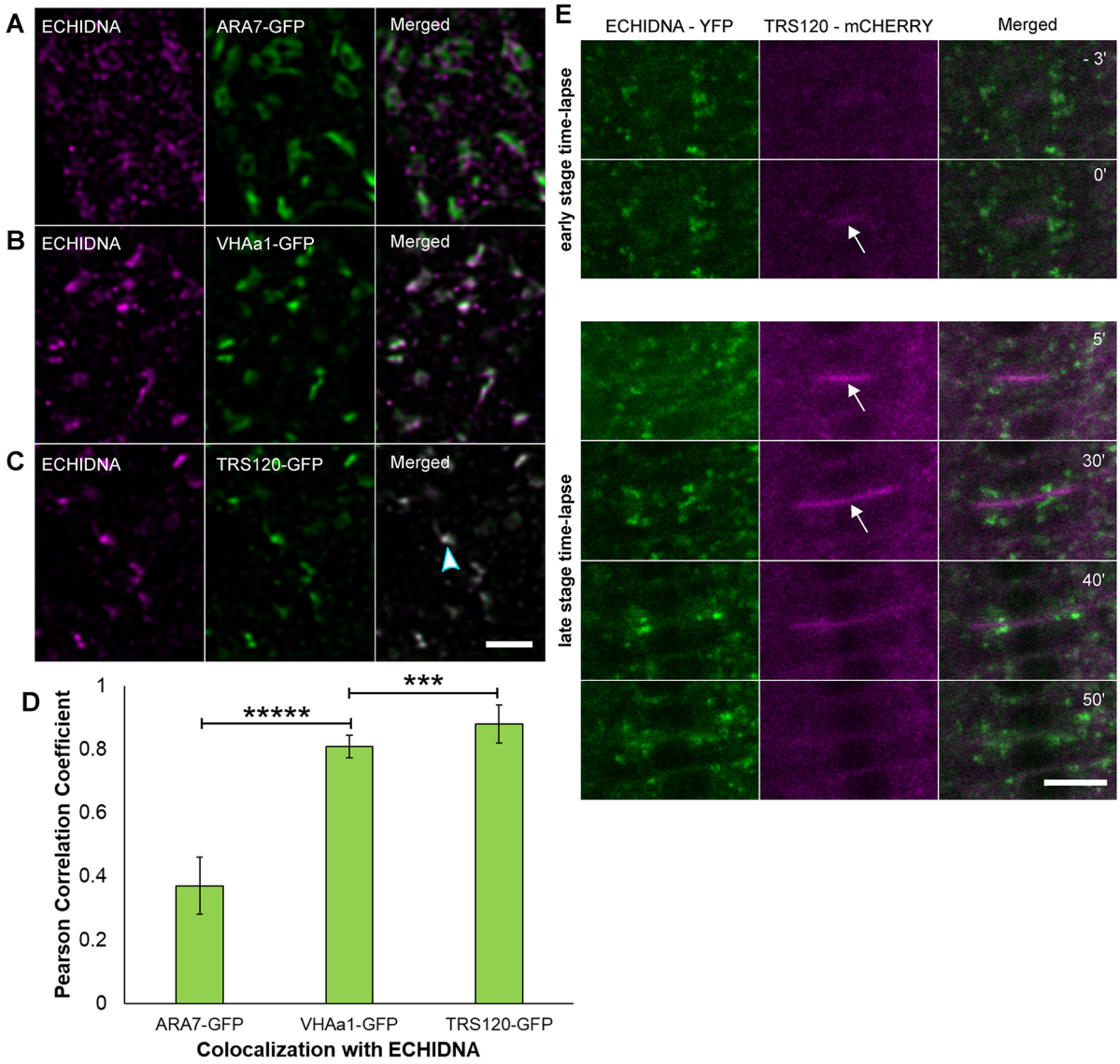

Fig. 1. Colocalization between ECHIDNA and TRS120-GFP in interphase and cytokinetic cells. (A-C) Confocal deconvolved and background-subtracted micrographs of fixed antibody stains. ECHIDNA (magenta) and GFP-labelled marker lines (green). Scale bar: 2 µm. (A) ECHIDNA and P_{35S}::ARA7-GFP. (B) ECHIDNA and P_{VHAa1}::VHAa1-GFP. (C) ECHIDNA and P_{TRS120}::TRS120-GFP. There is a strong degree of colocalization (arrowhead). (D) Pearson's correlation coefficient correlating ECHIDNA with ARA7-GFP, VHAa1-GFP and TRS120-GFP. The coefficient is based on the Costes' threshold. Data are mean ±s.d. Student's two tailed *t*-test ***$P<0.0003$; *****$P<10^{-6}$. Eight ARA7-GFP, 18 VHAa1-GFP and 13 TRS120-GFP cells were analyzed from at least three root tips per marker line. (E) Time-lapse (live imaging) of ECHIDNA-YFP and TRS120-mCherry, with minutes indicated in the right panel. Early and late stage time-lapses were imaged in two different cells of the same root tip. The numbers indicate minutes after the cell plate (arrows) becomes visible as a TRS120-mCHERRY-positive compartment. ECHIDNA-positive compartments accumulate around the cell plate but do not label it. A total of eight (partial) time lapse image series were captured. Scale bar: 10 µm.

2011; Qi et al., 2011). Here, we revisited this conclusion by carrying out a quantitative analysis of FM4-64 internalization dynamics (i.e. presence at the early endosome or TGN) at early time points in root tips. This showed that endocytosis was in fact impaired in all three mutants, but to different extents. Thus, in *echidna* and *club-2*, endocytosis was merely delayed, appearing near-complete 14 to 18 min after dye application (Fig. 3A,B). By contrast, in *trs120-4* mutants, endocytosis was severely impaired at all time points measured (Fig. 3B). This was surprising in light of previous claims that TRAPPII is not required for endocytosis (Qi et al., 2011).

In addition to its basal functions in secretion and anisotropic cell expansion, the TGN also has specialized functions in the establishment of polarity, cell differentiation, isotropic growth and cytokinesis. We monitored cell elongation and cytokinesis defects (i.e. incomplete cross walls) in mutant hypocotyls imaged via environmental s.e.m. This showed that *echidna* null mutants were impaired in cell elongation but not in cytokinesis (Fig. 3C,D). Conversely, *trappii* null mutants were impaired in cytokinesis but not in cell elongation (Fig. 3C-E). Like the difference in colocalization of the markers at interphase versus cytokinesis, these phenotypes point to a distribution of TGN functions among different players.

Plasma membrane markers are mislocalized to different compartments in *echidna* and *trappii* mutants

To monitor the role of ECHIDNA and TRAPPII in protein sorting, we first imaged two plasma membrane markers in wild-type versus mutant root tips. These were chosen on the basis of their

Development (2018) 145, dev169201. doi:10.1242/dev.169201

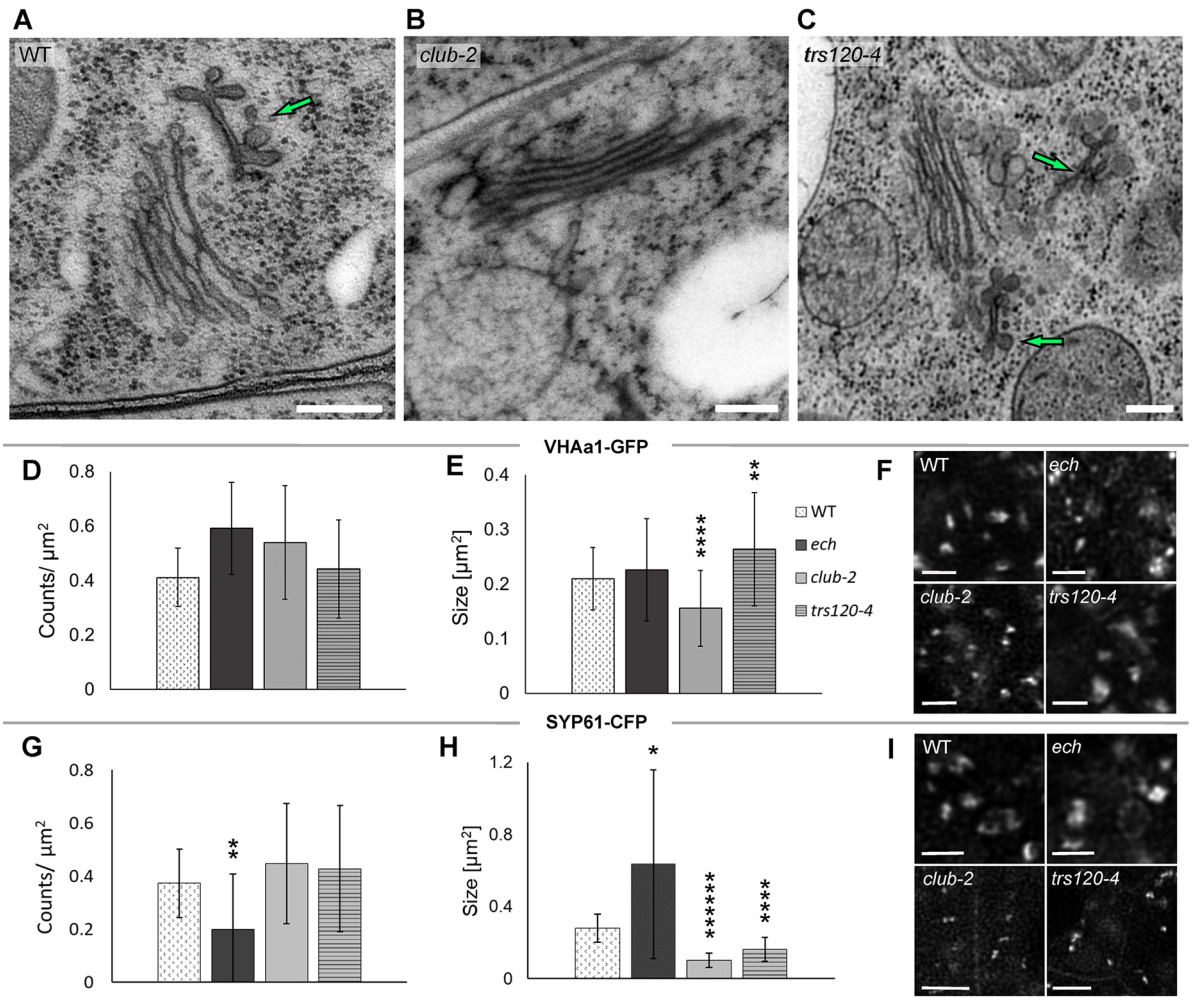

Fig. 2. TGN structure in *echidna* and *trappii* mutants. (A-C) TEM micrographs of wild-type (A), *club-2* (B) and *trs120-4* (C) cryofixed and freeze-substituted root tip cells. Arrows indicate canonical TGN-like structures in the wild type (A) and in *trs120-4* (C). We failed to detect TGN structures in *club-2* (B). The Golgi apparatus (GA) looked appressed in *club*-2 root tip cells (50.5% incidence; *n*=113 GA). Fifty-five GA were imaged for the wild type and 27 for *trs120-4*. Scale bars: 200 nm. (D-I) Comparison of normalized particle counts/cell area (D,G), average particle or aggregate size (E,H) and representative deconvolved CSLM micrographs (F,I) for TGN markers in wild type, *ech*, *club-2* and *trs120*-4. Data are mean±s.d. Student's two-tailed *t*-test: **P*<0.05, ***P*<0.01, *****P*<0.0001, ******P*<0.00001. Scale bars: 1.5 µm. (D-F) Behavior of P_{VHAa1}::VHAa1-GFP-positive compartments. In *echidna* mutants, particle or aggregate sizes were more variable than in the wild type. Particle size is decreased in *club-2* but particles aggregated in *trs120-4*; *n*=54 wild-type cells from 14 seedlings; *n*=37 *ech* cells from 10 seedlings; *n*=40 *club-2* cells from eight seedlings; *n*=57 *trs120-4* cells from 15 seedlings. (G-I) Behavior of P_{SYP61}::SYP61-CFP-positive compartments. Particle counts were decreased in *echidna* but unchanged in *trappii* mutants; conversely, particle size was increased in *echidna* and decreased in *trappii*. *n*=33 wild-type cells from 10 seedlings; *n*=18 *ech* cells from six seedlings; *n*=26 *club-2* cells from eight seedlings; *n*=23 *trs120-4* cells from six seedlings.

characteristic cell plate localization dynamics, which has been shown to be impaired in the *trappii* mutant *club-2* (Rybak et al., 2014), but which has not been studied in *echidna* and *trs120* mutants. SYP121-GFP (Collins et al., 2003) labels the plasma membrane and the cell plate throughout cytokinesis (Fig. 4A,E). In *echidna* mutants, plasma membrane and cell plate localization were observed as in the wild type. However, the majority of the SYP121-GFP signal resided on additional compartments that resembled vacuoles (Fig. 4B,E). In *club-2* mutants, SYP121-GFP localization was most severely impaired (Fig. 4C,E). In contrast, the behavior of SYP121-GFP in *trs120-4* resembled wild-type localization patterns during cytokinesis (Fig. 4E), yet endomembrane compartments were more abundant in non-dividing cells (Fig. 4D) of *trs120-4* compared with the wild type.

As a second plasma membrane marker, we imaged EXO84B-GFP, a subunit of the exocyst complex that is actively sorted away from the cell plate during the anaphase-to-telophase transition; it subsequently labels the cross wall after cell plate insertion and maturation (Fendrych et al., 2010; Rybak et al., 2014; Smertenko et al., 2017). This localization pattern was observed in *echidna* and in the majority of *trs120-4* cytokinetic cells but not in *club-2* mutants, where EXO84-GFP accumulated in slightly elongated endomembrane compartments (Fig. 4F). In conclusion, plasma membrane markers were mistargeted to different compartments in *echidna* and *club-2*. Indeed, we observed mistargeting of SYP61-CFP and of SYP121-GFP (but not EXO84b-GFP) to compartments resembling vacuoles in *echidna* but not in *trappii* mutant root tips (Fig. S2A; Fig. 4F). In addition, *club-2* mutants were more severely impaired in the targeting of plasma membrane markers than *trs120-4*.

Sorting to the cell plate is more severely impaired in *trappii* than in *echidna* mutants

To further our analysis of protein sorting in the different mutant backgrounds, we next imaged two TGN markers, VHAa1-GFP

Development (2018) 145, dev169201. doi:10.1242/dev.169201

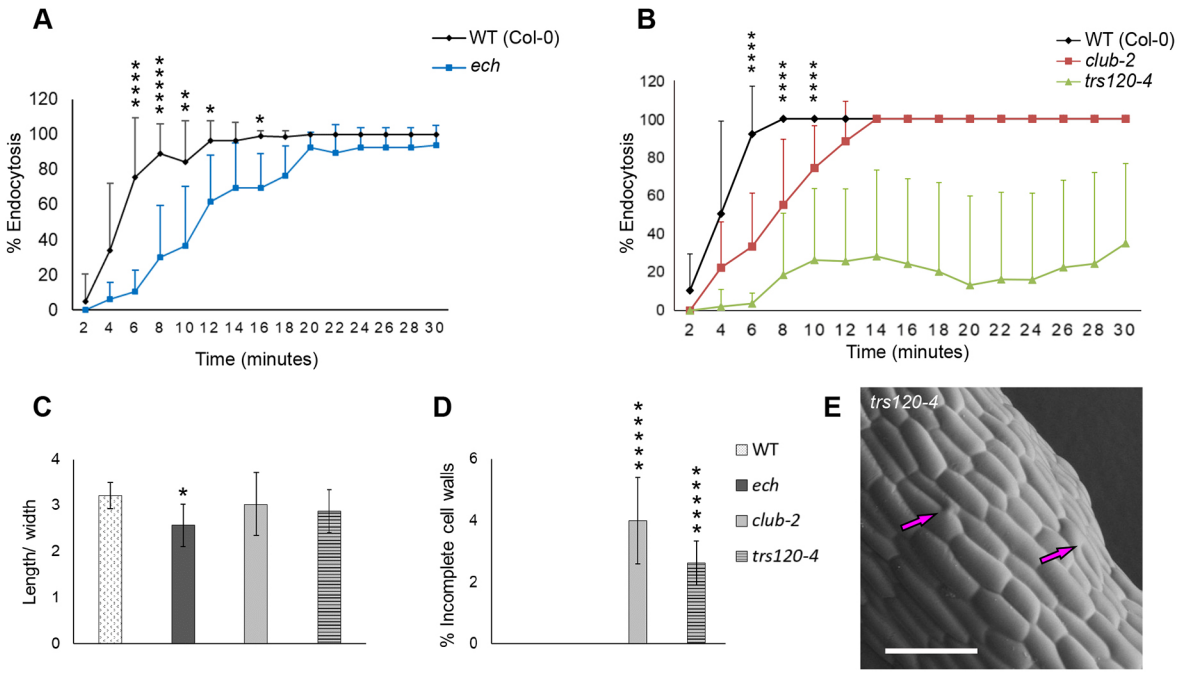

Fig. 3. Endocytosis, elongation and cytokinesis in *echidna* and *trappii*. (A,B) Rate of endocytosis, as computed by the number of FM4-64-positive vesicles per cell at the given time points. Data are mean±s.d. Student's two-tailed *t*-test: **P*<0.05, ***P*<0.01, *****P*<0.0001, ******P*<0.00001. (A) Endocytosis in *echidna* mutants. *n*=116 cells from 14 wild-type seedlings, *n*=84 cells from eight *echidna* seedlings. (B) Endocytosis in *trappii* mutants. *n*=225 cells from 16 wild-type seedlings, *n*=147 cells from 10 *club-2* seedlings, *n*=111 cells from eight *trs120-4* seedlings. (C,D) Cell elongation versus cytokinesis defects in *echidna* and *trappii* hypocotyls imaged by environmental scanning electron microscopy. Data are mean±s.d. Student's two-tailed *t*-test **P*<0.05, ******P*<0.00001. *n*=80 cells from five wild-type seedlings, *n*=175 cells from seven *echidna* seedlings, *n*=207 cells from nine *club-2* seedlings, *n*=162 cells from six *trs120-4* seedlings. (C) Cell elongation as measured by the length over the width of the cell. This is decreased in *echidna* (*P*=0.02) but not in *trappii* mutants. (D) Cytokinesis defects as measured by the incidence of cell wall stubs or incomplete walls. These are detected in *trappii* mutants ($P<10^{-04}$) but not in *echidna*. (E) Environmental scanning electron micrograph of a *trs120-4* seedling hypocotyl. Cell wall stubs are readily visible (arrows). Such stubs are not seen in the wild type. Scale bar: 100 µm.

and SYP61-CFP (Table S1), in mutant root tips throughout cytokinesis. VHAa1-GFP is a TGN marker that is predominantly excluded from the cell plate in the wild type (Fig. S3A; Dettmer et al., 2006). In *echidna* mutants, a weak cell plate localization was observed in 55% of cell plates (*n*=18; Fig. S3A arrows), which represents a subtle deviation from the wild type. In *trappii* mutants, the difference from the wild type was considerably stronger, with an aberrantly strong cell plate signal being observed in 89% (*n*=28) *club-2* and 72.2% (*n*=43) *trs120-4* cell plates (Fig. S3A arrows). In contrast to VHAa1-GFP, which is excluded from the cell plate in the wild type, SYP61-CFP labels the cell plate throughout cytokinesis and this pattern did not appear to be impaired in either *echidna* or in *trappii* mutants (Fig. S2B).

As the TGN markers above are either excluded from the cell plate or label it indiscriminately, we next imaged a bona fide cell plate marker: KEULE-GFP (Steiner et al., 2016b). KEULE-GFP is a cytosolic marker that is recruited to the cell plate at the onset of cytokinesis and labels this compartment throughout the cell cycle, being translocated to the rapidly expanding leading edges of the cell plate at the disc phragmoplast stage (Fig. S3B; Steiner et al., 2016a). The localization dynamics of KEULE-GFP at the cell plate differed from the wild type in *trappii* but not in *echidna* mutants, but there was less cytosolic signal in *echidna* than in the wild type (Fig. S3B). Furthermore, and in contrast to plasma membrane markers, *trs120-4* mutants were more severely impaired in the targeting of a cell plate marker than *club-2*. In conclusion, protein sorting at the cell plate was impaired in *trappii* but not in *echidna* mutants.

An analysis of physical, network and genetic interactions suggests that ECHIDNA and TRAPPII belong to distinct overlapping pathways

To assess the nature of a possible functional interaction between ECHIDNA and TRAPP subunits, we first tested for a physical interaction. Immunoprecipitation followed by mass spectrometry with TRAPPII-specific GFP fusion proteins *in planta* (as described by Rybak et al., 2014) failed to detect any physical interaction with either ECHIDNA or YIP proteins (F.F.A. and B. Küster, unpublished). Consistently, pairwise yeast-two-hybrid tests with all eight TRAPPII subunits (or truncations thereof) as baits and with ECHIDNA and YIP4b as prey revealed no evidence for interactions. However, all eight TRAPPII subunits, as well as ECHIDNA and YIP4b, do interact with other partners in our system (Arabidopsis Interactome Mapping Consortium, 2011; Steiner et al., 2016b, not shown). In light of this negative interaction data in very well controlled settings, we deployed a network approach. We had previously mapped an *Arabidopsis* protein-protein interactome network, describing 6200 interactions among 2700 proteins and identifying 26 network communities of proteins that are more highly connected to each other than to the rest of the network; of these, 23 are enriched in functionally consistent gene ontology annotations (Arabidopsis Interactome Mapping Consortium, 2011). Importantly, ECHIDNA and two core-TRAPP subunits (Table S3) were included in this systematic network mapping experiment, which allowed us to investigate their relative position in the local and global network neighborhood. ECHIDNA is a member of the large 'transmembrane transport' community (Fig. 5). In contrast, two core-TRAPP subunits are outside any detectable community in

Development (2018) 145, dev169201. doi:10.1242/dev.169201

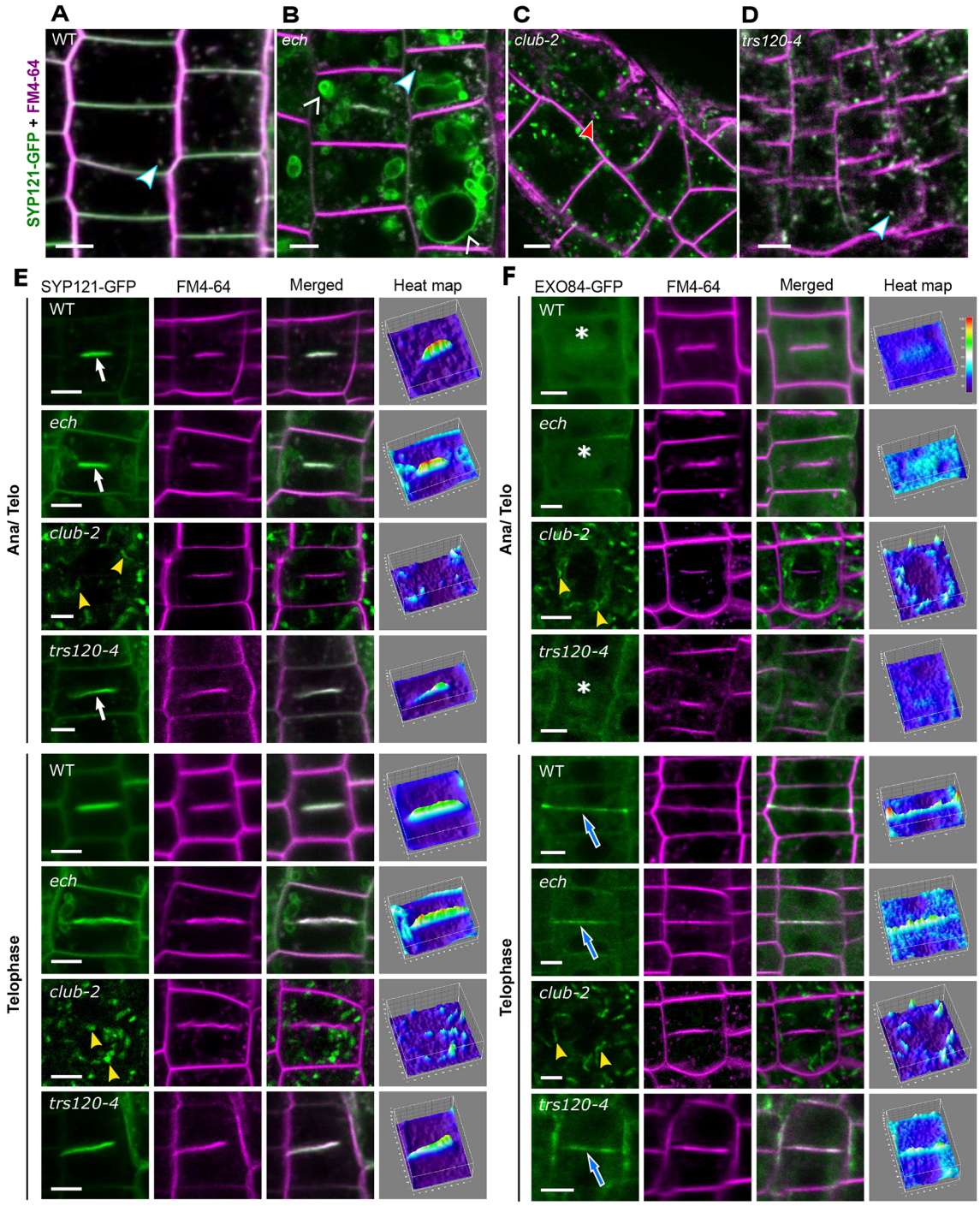

Fig. 4. Sorting of plasma membrane markers in *echidna* and *trappii* root tips. Live imaging with GFP marker in green and FM4-64 in magenta. Scale bars: 5 µm. (A-D) P_{SYP121}::SYP121-GFP in non-dividing cells. SYP121-GFP-positive vesicles colocalize with FM4-64 in all backgrounds (blue-rimmed white arrowheads) with the exception of *club-2* (white-rimmed red arrowhead in C). There is mistargeting to vacuole-like structures in *echidna* (arrowheads in B). *n*=38 wild-type, *n*=7 *ech*, *n*=10 *club-2* and *n*=11 *trs120-4* seedlings. (E,F) Imaging of cytokinetic cells. Surface plots are 3D heat maps depicting fluorescence intensity along the *z*-axis with a scale ranging from blue (low) to red (high). Arrows indicate cell plates; yellow arrowheads indicate deviant vesicles in *club-2*. (E) P_{SYP121}::SYP121-GFP. *n*=52 wild type, *n*=17 *ech*, *n*=12 *club-2*, *n*=28 *trs120-4* cytokinetic cells from at least ten seedlings. (F) P_{EXO84}::EXO84B-GFP. Asterisk indicates a diffuse cloud of GFP signal around the cell plate prior to insertion into the lateral wall; the white-rimmed blue arrow indicates a cross wall. *n*=13 wild type, *n*=15 *ech*, *n*=11 *club-2*, *n*=10 *trs120-4* cytokinetic cells from at least ten seedlings.

the global network and on the cytosol-proximal side of the 'vesicle trafficking' community (Fig. 5). The shortest path between ECHIDNA and core-TRAPP has a length of six nodes and spans two communities (Fig. 5). Of the 30 TGN-resident proteins (Groen et al., 2014), five are members of the transmembrane transport community; none belongs to the vesicle trafficking community. These data provide network level evidence for the involvement of ECHIDNA and TRAPP in two separate yet adjacent pathways.

The network interactions suggest that ECHIDNA and TRAPPII may act in distinct pathways. To assess whether these are partially

Development (2018) 145, dev169201. doi:10.1242/dev.169201

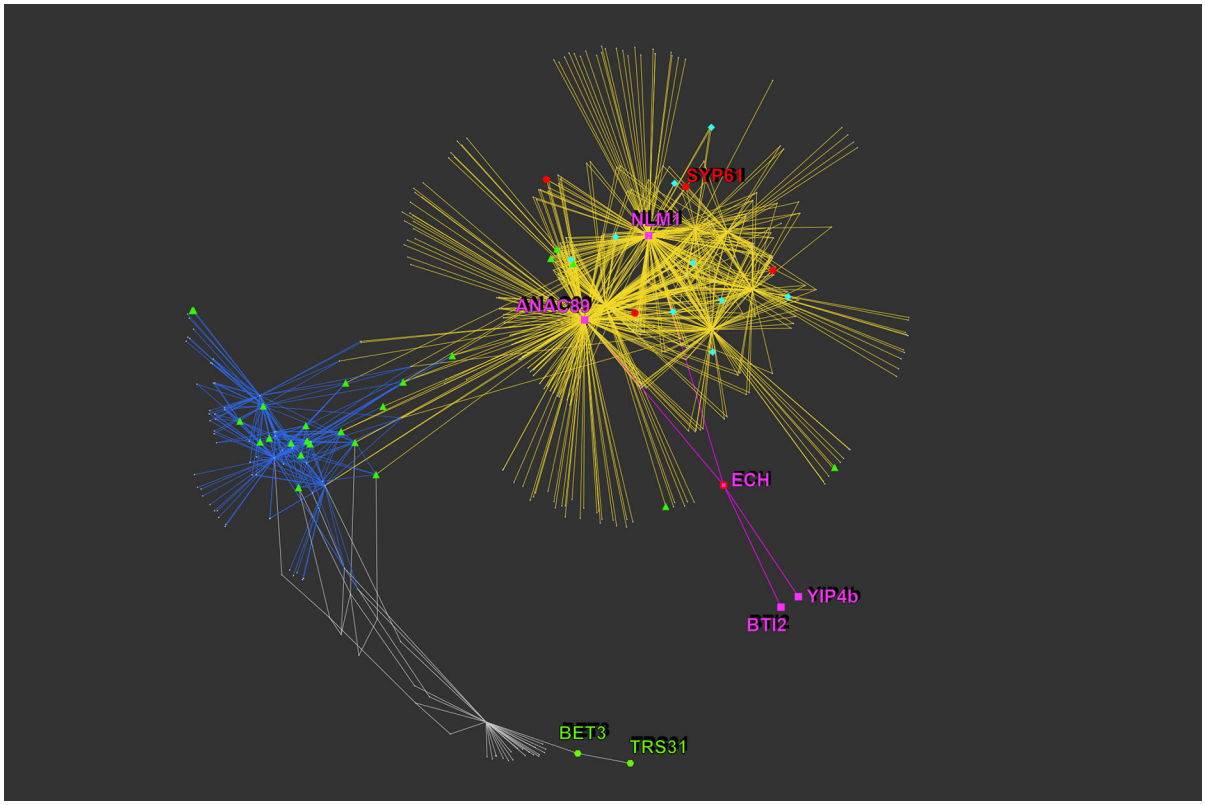

Fig. 5. Projection of core-TRAPP subunits and ECHIDNA onto the *Arabidopsis* Interactome Map. ECHIDNA (ECH) is associated with the 'transmembrane transport community' (yellow lines or edges), whereas core-TRAPP subunits (green circles) are most closely associated with the 'vesicle trafficking community' (blue lines or edges) (Arabidopsis Interactome Mapping Consortium, 2011). Two of the four ECHIDNA interactors (magenta squares, ANAC89 and NLM1) are central nodes in the transmembrane transport community, which is more than tenfold enriched in proteins possessing transporter activity (P=1.4 e-^{31}). GTPases and related proteins (green triangles) are more than 15-fold enriched in the vesicle trafficking community (P=2.6 e^{-08}) and at the intersection between the two communities. Red circles indicate TGN resident proteins (Groen et al., 2014). Proteomic analyses link the TRAPPII-specific subunit AtTRS120 to the transmembrane transport community via interactions with SYP61 (Drakakaki et al., 2012). Turquoise diamonds indicate members of the SNARE interactome (Fujiwara et al., 2014). Both the TGN and SNARE interactome proteins map to the transmembrane transport community.

redundant or independent, we performed double mutant analysis. In the case of an independent interaction, an additive double mutant phenotype would be predicted. In case of partial redundancy or overlap, a synthetically enhanced or synergistic (i.e. more than additive) double mutant phenotype would be predicted. We first noticed that the incidence of collapsed seed, which is indicative of embryo lethality, increased more than tenfold (P=0.01) among the progeny of plants homozygous for *echidna* (*ech*) and segregating *trappii* null alleles (Fig. S4A,B). We then monitored embryo phenotypes in the siliques of plants segregating single or double mutant progeny. *echidna* single mutants had only weak embryo phenotypes up to heart stages (Fig. 6A and Fig. S4C), whereas *club-2* and *trs120-4* single mutants exhibited some aberrant cell divisions throughout embryogenesis, at an average frequency of 11.8% for *club-2* (Fig. 6A; n=511 embryos) and of 10.6% for *trs120-4* (Fig. S4C; n=254 embryos). Among the progeny of plants homozygous for *echidna* and segregating *trappii* null alleles, we observed a high incidence of aberrant embryos until the heart stage; the deviations from the wild type were particularly visible in the basal region of the embryo and affected the root primordia (Fig. 6A; Fig. S4C). Furthermore, reduced cell elongation gave rise to radially swollen embryos (Fig. 6A). At the heart stage, the incidence of double mutants dropped and by the torpedo stage we observed none at all (0%, n=130 torpedo stage mutants for the *ech club-2* double mutant; compare with 13%, n=54 *club-2* torpedo embryos). Together with the synergistically increased incidence of collapsed seed, we inferred that double mutant embryos are lethal, collapsing by the late heart stage.

In brief, the combination of a viable *echidna* allele with seedling lethal *trappii* alleles gave rise to embryo lethality. Similarly, combining two viable alleles of *echidna* and *trappii* gave rise to seedling lethality: double mutants between *echidna* and a viable hypomorphic (or weak) *trs120* allele, *trs120-5* (Table S2), were severely dwarfed non-viable seedlings with isodiametric cells (Fig. 6B; Fig. S5). We conclude that the double *ech trs120* or *ech club-2* mutants had a synthetically enhanced or synergistic phenotype. To establish which specific trait(s) was (were) synthetically enhanced in the double mutants, we conducted a cellular analysis of single versus double mutant phenotypes. A survey of 15 antibodies revealed Arabinogalactan protein (AGP) glycans as excellent markers for secretion; these are complex structures assembled at the ER and Golgi and transported to the cell wall via secretory vesicles (Nguema-Ona et al., 2014). AGP glycans labeled the cell wall in *echidna* and null *trappii* mutants but utterly failed to accumulate at the cell surface in *echidna trs120-5* double mutants (Fig. 6C; a null *trs120* allele was used for the single mutant but a hypomorphic *trs120* allele was used for the double mutant). Cell elongation was also synthetically impaired in the double mutants (Fig. 6D). We conclude that there was a synthetic enhancement of the secretion defect and of cell elongation in the double mutant embryos or seedlings.

Development (2018) 145, dev169201. doi:10.1242/dev.169201

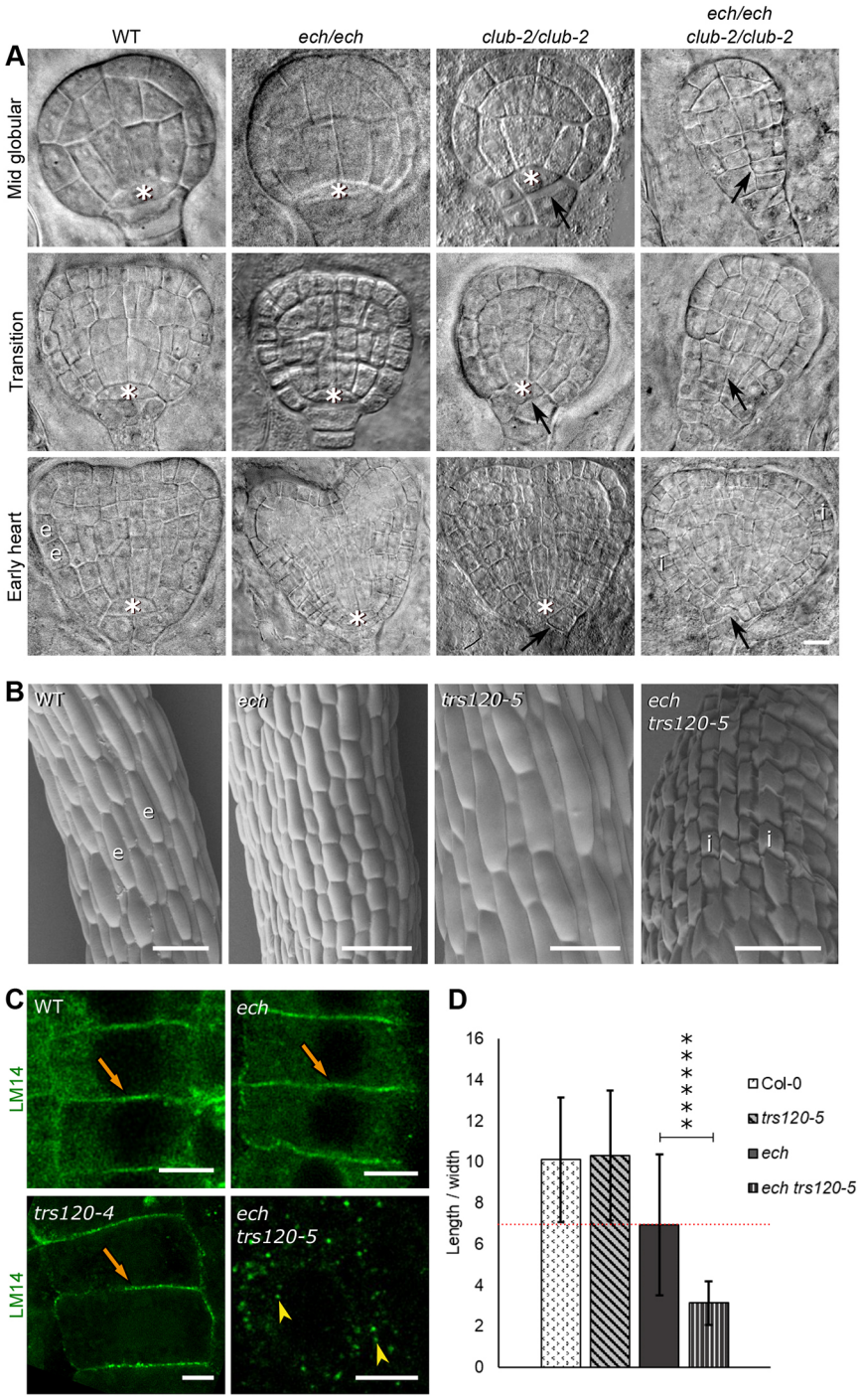

Fig. 6. Double mutant analysis between *echidna* and *trappii*. (A) Embryogenesis in *echidna* and *club-2* single and double mutants. Null alleles used for both loci. Asterisk indicates the hypophysis or its progeny. Black arrows indicate aberrant cell division planes. Isodiametric cells and radial swelling occur in *ech club-2* heart stage double mutants (bottom right panel). e, elongated cell; i, isodiametric cell. *n*=157 embryos from three wild-type mother plants, *n*=123 embryos from three *ech* mother plants, *n*=511 embryos from six *club-2* mother plants, *n*=162 embryos from seven *ech club-2* mother plants. Scale bar: 10 µm. (B) Environmental scanning electron micrographs (SEMs) of hypocotyl cells. Null allele for *echidna*; hypomorphic allele *trs120-5* for *trs120*. Isodiametric collapsed cells are present in the *ech trs120-5* double mutant. e, elongated cell; i, isodiametric cell. Scale bars: 100 µm. (C) Antibody staining of root tips with LM14 antibody against AGP glycans. The polysaccharide is secreted to the cell surface (orange arrows) in the wild type and null single mutants, but it accumulates in intracellular vesicles (yellow arrowheads) in the *ech trs120-5* double mutant. *n*=8 wild-type seedlings; *n*=6 *ech* seedlings; *n*=7 *trs120-4* seedlings; *n*=6 *ech trs120-5* seedlings. Scale bars: 5 µm. (D) Cell elongation in the root tip of single versus double mutants. Cell elongation is affected in *echidna*-null but not in *trs120-5* hypomorphic alleles; it is synthetically (i.e. more than additively) enhanced in the *ech trs120-5* double mutant. Data are mean±s.d. Student's two-tailed *t*-test. ******$P<e^{-29}$. Ten seedlings were analyzed per genotype. *n*=41 wild type, *n*=40 *ech*, *n*=30 *trs120-5* and *n*=59 *ech trs120-5* cells.

In light of the genetic interaction between the genes, we sought to establish whether there was any mutual dependence with respect to localization patterns. To achieve this, we monitored the behavior of TRAPPII in *echidna* and vice versa. The TRAPPII TRS120-GFP marker exhibited normal cell plate localization dynamics in *echidna* mutants (Fig. 7A). Furthermore, the number and appearance of TRS120-GFP positive compartments were indistinguishable between *echidna* and the wild type during interphase (Fig. 7B-D). Similarly, the appearance of ECHIDNA was not affected by *trappii* mutation (Fig. 7E-G). In addition, the colocalization coefficient of VHAa1-GFP with respect to ECHIDNA was not affected in *trappii* mutants (Fig. 7H). Remarkably, even in *trappii* cytokinetic cells in which the VHAa1-GFP TGN marker was mistargeted to the cell plate, ECHIDNA was excluded from the cell plate, as in the wild type (Fig. 7I; compare with Fig. 1E). We conclude that the localization patterns of ECHIDNA and TRAPPII are not dependent on each other. Taken together, our data suggest that ECHIDNA and TRAPPII act in independent pathways that are capable of compensating for each other with respect to essential TGN functions such as secretion.

DISCUSSION

The TGN is a key trafficking compartment mediating secretion to the plasma membrane, vacuolar targeting and endocytosis. As a result, the TGN has a profound impact on cell growth and

Development (2018) 145, dev169201. doi:10.1242/dev.169201

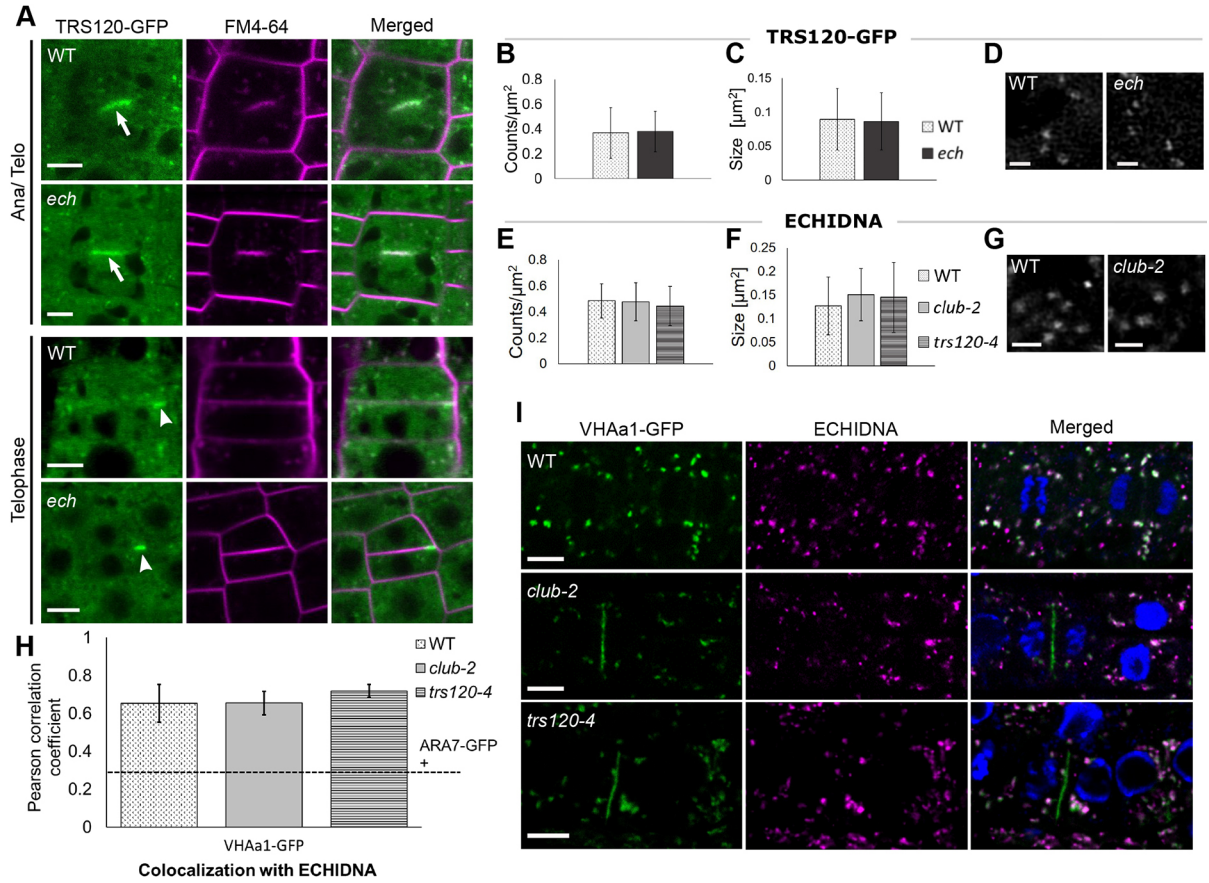

Fig. 7. Behavior of TRS120-GFP in *echidna* and of ECHIDNA in *trappii* mutants. (A) Live imaging of P_{TRS120}::TRS120-GFP in wild-type and *echidna* root tip cells. The mutant and wild-type localization dynamics are similar. Two partial and two complete time lapses were performed. Scale bars: 5 µm. (B-G) Comparison of normalized particle counts/cell area (B,E), average size of particles or aggregates (C,F) and representative CSLM deconvolved images (D,G) for TRS120-GFP live (B,C) (*n*=28 wild-type cells from seven seedlings; *n*=29 *ech* cells from eight seedlings) or ECHIDNA antibody (E-G) signal in segregating wild type and mutants (*n*=35 cells from five wild-type seedlings, *n*=52 cells from 19 *club-2* seedlings, *n*=64 cells from 12 *trs120-4* seedlings). Interphase cells were chosen for analysis. Single cells were selected as region of interest for the experiment. Data are mean±s.d. Student's two-tailed *t*-test. Scale bars: 1.5 µm. (H) Average Pearson's correlation coefficient for ECHIDNA with VHAa1-GFP in wild type and mutants. The dotted line indicates the average Pearson's correlation coefficient for ECHIDNA with ARA7-GFP in the wild type. The colocalization of ECHIDNA with VHAa1-GFP was assessed in *trappii* mutants. Images were deconvolved, background subtracted and a region of interest selected. Shifts between wild type and mutant were insignificant (P>0.066). *n*=14 wild type, *n*=10 *club-2*, *n*=6 *trs120-4* cells, each from a different seedling. (I) Antibody stains of ECHIDNA and VHAa1-GFP in wild-type and *trappii* root tips. Anti-GFP (green); anti-ECHIDNA antibody (magenta); DAPI/nucleus (blue). In *trappii* mutants, VHAa1-GFP is mislocalized but ECHIDNA is not. Scale bars: 5 µm.

differentiation. In a multicellular context, cells in an organ are often found to be in different developmental or cell cycle stages, which places different demands on TGN function. Here, we have compared interphase versus dividing cells and investigated how the TGN mediates trafficking in these cells by examining ECHIDNA and the TRAPPII tethering complex, both having been implicated in TGN structure and function. STED super-resolution microscopy failed to resolve ECHIDNA and TRAPPII into different structures in interphase cells, suggesting that they are in close proximity in non-dividing cells. In contrast, live imaging of dividing cells revealed that their localization dynamics differed during cytokinesis: tagged TRAPPII subunits labelled the cell plate, whereas ECHIDNA did not. Consistently, *echidna*-null mutants were impaired in cell elongation but not in cytokinesis, whereas *trappii* null mutants were impaired in cytokinesis but not in cell elongation. In addition, protein sorting at the cell plate was considerably more impaired in *trappii* than in *echidna* mutants (Fig. 8). Our findings indicate that *echidna* and *trappii* mutants have a measurable but different impact on TGN structure and function; endocytosis, for example, was impaired in both *echidna* and *trappii* mutants, but to different extents (Fig. 8). Plasma membrane markers were mistargeted to different compartments in *echidna* and *trappii* mutants. An analysis of physical, network and genetic interactions suggests that ECHIDNA and TRAPPII act in parallel yet overlapping pathways. Thus, while they appear to be partially redundant with regard to basal TGN functions, such as secretion in interphase cells, ECHIDNA and TRAPPII have distinct specialized functions. Cell plate biogenesis, for example, required TRAPPII but not ECHIDNA.

We failed to identify direct or indirect physical interactions between the TRAPPII octomeric complex and ECHIDNA or YIP4a/b, Rab GTPase-binding ECHIDNA interaction partners (Gendre et al., 2013; Yang, 1998). ECHIDNA has four binary interaction partners in our yeast-two-hybrid system, including YIP4b (Arabidopsis Interactome Mapping Consortium, 2011). Furthermore, when core-TRAPP subunits and ECHIDNA, together with their binary interactors, are projected onto the *Arabidopsis* Interactome map (Arabidopsis Interactome Mapping Consortium, 2011), they are associated with or belong to different communities. ECHIDNA is a member of the transmembrane transport

Development (2018) 145, dev169201. doi:10.1242/dev.169201

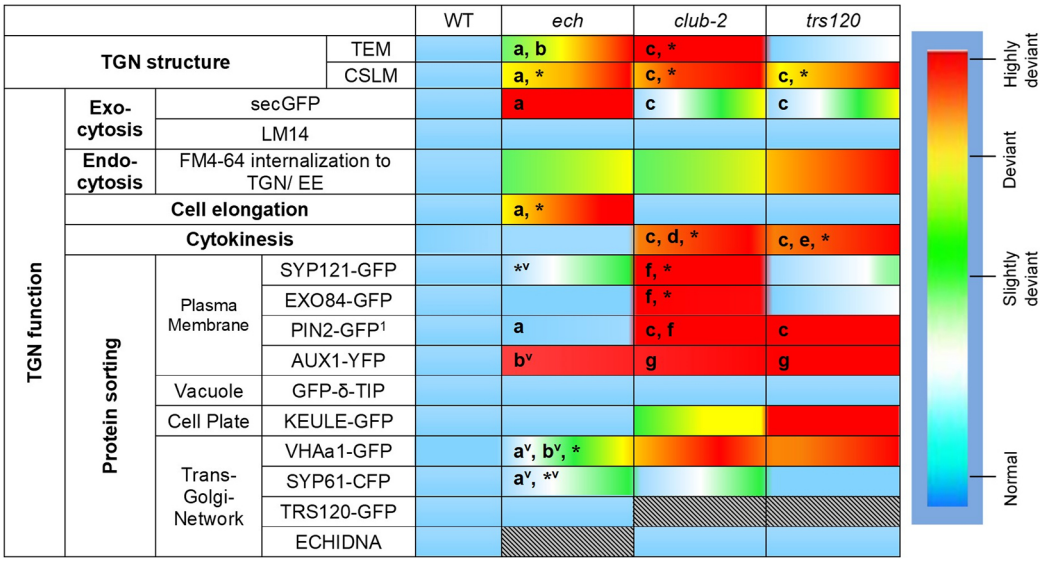

Fig. 8. TGN structure and function in *echidna* and *trappii*. The heat map depicts the extent of deviation from the wild type (see scale), with gradients representing the range of phenotypes observed. Grey rectangles with lines indicate that this data point does not apply. The data summarize the observations of this study, unless otherwise specified. (a) Gendre et al. (2011); (b) Boutté et al. (2013); (c) Qi et al. (2011); (d) Jaber et al. (2010); e: Thellmann et al. (2010); f: Rybak et al. (2014); g: Qi and Zheng (2011). Asterisk indicates also reported in this study. [1]Immunostaining for *echidna*, live imaging of GFP marker for *trappii*. v indicates the vacuolar mislocalization of marker, seen specifically in *ech* mutants.

community, which is enriched in diverse transporters, and contains TGN-resident proteins (Groen et al., 2014) and SNARE interactors (Fujiwara et al., 2014). Furthermore, two ECHIDNA interactors, an aquaporin and a membrane-tethered transcription factor, are central hubs in the transmembrane transport community (see Fig. 5 and Table S4).

Core-TRAPP components are two network steps away from the cytosolic side of the vesicle trafficking community, which is enriched in small GTPases or related proteins such as prenylated Rab acceptors or GDP dissociation inhibitors (Arabidopsis Interactome Mapping Consortium, 2011). This is consistent with our understanding of TRAPP function on two fronts: first, TRAPPII is TGN-associated but predominantly cytosolic (Rybak et al., 2014); and second, in yeast and mammals the best documented function of TRAPP complexes is to act as guanine-nucleotide exchange factors (GEFs) for Rab GTPases. GEFs catalyze exchange of GDP for GTP; the GTP-bound, activated Rab subsequently recruits a diverse local network of Rab effectors to the membrane to give it identity in vesicle fusion events (Barr, 2013; Kim et al., 2016). In *Arabidopsis*, the TRAPPII tethering complex is thought to be a GEF for the Rab-A family of GTPases (Qi and Zheng, 2011; Qi et al., 2011; Ravikumar et al., 2017). With 26 members, the plant Rab-A GTPase family is vastly expanded and diversified (Rutherford and Moore, 2002; Vernoud et al., 2003). TRAPPII-Rab interactions are bound to play crucial roles in organizing membrane traffic (Barr, 2013; Kim et al., 2016) and are thought to mediate the selective delivery, retention and retrieval processes that characterize cell plate progression-maturation (Ravikumar et al., 2017). Similarly, TRAPPII-Rab interactions likely underlie the sorting decisions depicted in this study. The cell plate is a RabA2/A3 compartment (Chow et al., 2008) and it will be interesting to see whether TRAPPII acts as a GEF for this subclass of Rab GTPases during cytokinesis, but as a GEF for other Rab GTPases to modulate other specialized TGN functions. RabA5c, for example, has a unique localization pattern at the geometric edges of cells (Kirchhelle et al., 2016); whether it is differentially activated by TRAPPII to mediate anisotropic growth and cell patterning during *Arabidopsis* organogenesis is an unanswered question.

Proteomic analyses link the TRAPPII-specific subunit AtTRS120 to the transmembrane transport community via interactions with SYP61 (Drakakaki et al., 2012). Interestingly, the interface between the vesicle trafficking and transmembrane transport communities is, like the vesicle trafficking community, also enriched in GTPase-related proteins (Fig. 5). In addition, ECHIDNA has been shown to interact genetically with ARF1 GTPases and BIG ARF-GEFs (Jonsson et al., 2017). ARF GTPases are required for vesicle budding and it is tempting to speculate that ECHIDNA, ARF1 and BIG ARF GEFs operate in concert for the genesis of secretory vesicles at the TGN. In yeast-two-hybrid screens, ECHIDNA also interacts with YIP proteins, the yeast and mammalian homologs of which are known to physically interact with Rab GTPases (Fig. 5; Gendre et al., 2013). Elegant chemical genomic approaches have suggested that Rab GTPases work in concert with BIG ARF-GEFs to modulate distinct endomembrane sorting routes that are essential for the establishment of cell polarity (Li et al., 2017; Robert et al., 2008).

The localization to or association with different communities in the *Arabidopsis* Interactome map is consistent with the considerable differences we observe between TRAPPII and ECHIDNA (Fig. 8). The difference in localization dynamics during cytokinesis shows how TGN subcompartmentalization is regulated in a dynamic fashion, possibly by cell cycle cues. The TRAPPII complex is linked to both the nuclear cycle and to mitotic microtubule arrays via a link with PLEIADE/AtMAP65-3 (Steiner et al., 2016a). Indeed, MAP65 proteins are targets of cell cycle-regulated kinases (Kosetsu et al., 2010; Sasabe et al., 2011a,b)). The TRAPPII-MAP65 interaction would thereby transmit cues pertaining to cell cycle progression to the trafficking apparatus at the cell plate, guiding cell plate biogenesis and expansion in response to cell cycle cues. There are no reports of ECHIDNA function being regulated by the cell cycle, and this possible difference may underlie the

Development (2018) 145, dev169201. doi:10.1242/dev.169201

differential responsiveness of ECHIDNA and TRAPPII to cell cycle progression during mitosis. Such a differential responsiveness could explain how developmental cues regulate the cargo composition and sorting of TGN vesicles, and how specialized TGN functions are differentially regulated by different cues.

The network interactions suggest that ECHIDNA and TRAPPII may act in distinct pathways. Double mutant analysis was conducted to assess whether these are partially redundant or independent. ECHIDNA and TRAPPII exhibit a synergistic genetic interaction. Synergy often points to parallel pathways and also suggests that ECHIDNA and TRAPPII are at least partially functionally redundant (Pérez-Pérez et al., 2009). Double mutant embryos or seedlings had enhanced phenotypes with respect to cell elongation and to the secretion of cell wall polysaccharides. Secretion to the plasma membrane occurs through a variety of different routes, as evidenced by the observation that both ECHIDNA and TRAPPII are required for the delivery of some proteins to the plasma membrane but not of others (Gendre et al., 2015; Rybak et al., 2014). AUX1-YFP localization, for example, is affected in both *echidna* and *trappii*, whereas PIN2-GFP polarity is affected in *trappii* but not in *echidna* (Gendre et al., 2015; Qi et al., 2011; Rybak et al., 2014). A plausible interpretation of the synergies we observe is that ECHIDNA and TRAPPII mediate different but overlapping routes to the plasma membrane, and that the secretion of certain forms of cargo is abolished in the double mutants, as observed for AGP glycans. Two parallel pathways able to compensate for each other might explain why null *echidna* or *trappii* alleles survive until or past the seedling stage; it would also contribute to the robustness of TGN essential basal functions.

We set out to compare *echidna* and *trappii* and, to our surprise, found that the difference between the two TRAPPII-specific subunits AtTRS120 and AtTRS130/CLUB were at times larger than differences between *echidna* and *trappii* (Fig. 8). This was surprising in light of previous claims that the two TRAPPII-specific subunits are interchangeable (Qi et al., 2011). Furthermore, AtTRS120 and AtTRS130/CLUB have been shown to be subunits of the same complex in *Arabidopsis* (Rybak et al., 2014). The molecular basis for the differences between the two TRAPPII-specific subunits remains unclear, and its elucidation is not within the scope of this study. Nonetheless, the difference between the two subunits is likely to add different layers of complexity and fine-tuning to TGN function. This would represent one more manifestation of the complexity of post-Golgi trafficking in plants. Whereas the largest SNARE and Rab GTPase families are mostly TGN related (Chow et al., 2008; Kirchhelle et al., 2016; Sanderfoot et al., 2000), a recent report reveals sophisticated regulatory mechanisms for late endosomal Rab GTPases (Ito et al., 2018).

In conclusion, the analysis of ECHIDNA and the TRAPPII proteins provide new insights into the differential and dynamic organization of the plant TGN. The distinct TGN compartments we describe here were not distinguishable during interphase. They only became apparent at the onset of cytokinesis, when the TRAPPII subunit labeled the cell plate, whereas ECHIDNA did not. Thus, it appears that cell cycle cues have differential impacts on these TGN components, which differentially affect specialized TGN functions such as cell plate biogenesis and anisotropic growth. In addition, we show that ECHIDNA and TRAPPII are independent of each other for their localization. Indeed, *trappii* cells in which VHAa1 is mislocalized have a proper ECHIDNA localization. Two independent pathways able to compensate for each other would contribute to the robustness of TGN essential basal functions as well as to the responsiveness and fine tuning of its specialized functions. The study of ECHIDNA and TRAPPII offers novel molecular handles on the partitioning of TGN functions. Future studies will help elucidate how these key players are differentially regulated by diverse developmental, cell cycle or environmental cues.

MATERIALS AND METHODS

Lines and growth conditions

All the lines used in this study are listed in Table S2. Seedling-lethal mutants were propagated as hetero- or hemi-zygotes. Insertion lines were selected via the TAIR and NASC websites (Swarbreck et al., 2008). Plants were grown in the greenhouse under controlled temperature conditions and with supplemental light, or under controlled growth chamber conditions (16/8 h photoperiod at 250 µmol m^{-2} s^{-1}). Seedlings were surface sterilized, stratified at 4°C for 2 days and plated on MS medium supplemented with 1% sucrose and B5 vitamins (Sigma). The root tips or hypocotyls of 5-day-old plate-grown seedlings were used for light, confocal and electron microscopy. For an analysis of embryogenesis in double mutants, we dissected the mature siliques of plants homozygous for *echidna* and segregating the *trappii* T-DNA insertion (as verified by PCR analysis).

Antibody stains and confocal microscopy

Immunolocalizations were carried out as described by Rybak et al. (2014) with anti-ECHIDNA (rabbit, 1:600; Gendre et al., 2011) or anti-GFP (mouse, 1:1000, Abcam) as primary antibodies for the GFP-tagged proteins. Polysaccharide antibodies included LM14 (rat monoclonal, 1:10, Plant Probes). Secondary antibodies were anti-rabbit monoclonal Alexa-m488 (goat, 1:600, Molecular Probes), anti-mouse Cy3 (goat, 1:600, Dianova) and anti-rat Alexa-m488 (goat, 1:100, Molecular Probes). Nuclei were stained with 1 µg/ml DAPI (Sigma). Cell cycle stage was determined by nuclear stage for antibody stains and via time lapses in live imaging.

Confocal microscopes used for imaging were: (1) an Olympus (www.olympus-ims.com) Fluoview 1000 confocal laser scanning microscope (CSLM); (2) a Leica (www.leica-microsystems.com) SP8 Hyvolution CSLM; and (3) an Axioplan inverted microscope with a Zeiss (www.zeiss.com) LSM 780 spectral CSLM.

STED imaging was performed on a combined Abberior STED and RESOLFT Expert Line system (Abberior Instruments) operated by the software Imspector (Abberior Instruments). Samples were imaged with an Olympus 100×/NA1.4 UPLANSAPO oil immersion objective on an Olympus IX83 stand using a 775 nm pulsed depletion laser (Olympus). A typical donut-shaped depletion pattern was used for 2D STED super-resolution microscopy, enhancing the resolution laterally to ∼50-70 nm. Dual-color images were recorded in line-sequential mode on separate APDs with 605-625 nm and 650-720 nm bandpass matching the fluorophores Abberior Star 600 and Abberior Star 635P (Abberior), respectively. GFP-tagged proteins were stained with FluoTag X4 anti-GFP AbberiorStar635p (E. *coli*, 1:250, NanoTag Biotechnologies) and we used AbberiorStar600 anti-rabbit (goat, 1:600, Abberior) as a secondary antibody; Star600 was excited with a 594 nm and Star635 with a 644 nm laser. See supplementary Materials and Methods for further information regarding the primary antibodies.

Image processing and analysis

Images taken with the Leica SP8 microscope were deconvolved using the built-in Huygens Scientific deconvolution software (www.leica-microsystems.com) operated in both 2D and 3D. For colocalization analyses, images were deconvolved using the Huygens Essential software and then background subtracted using a top-hat filter (radius: 25 pixel); the ImageJ plug-in JACoP (Bolte and Cordelières, 2006) was used to calculate the Pearson's correlation coefficient based on the Costes' threshold (Costes et al., 2004). For consistency in quantitative analyses, we selected cortical root tip cells, at a height of 6-22 cells above the quiescent center in the root apical meristem.

Histological sections and light microscopy

Embryos were harvested, fixed, infiltrated, embedded and imaged as described previously (Matthes and Torres-Ruiz, 2016). The molecular techniques used to genotype the double mutant by PCR analysis of both

insertion alleles are described in the supplementary Materials and Methods.

Electron microscopy

For scanning electron microscopy, a Zeiss (LEO) VP 438 microscope was operated at 15 kV. Fresh seedlings were placed onto stubs and examined immediately in low vacuum. Seeds were sputtered with platinum and imaged in high vacuum. A Zeiss EM912 Omega microscope was used for transmission electron microscopy. Cryofixation and freeze substitution protocols are described in the supplementary Materials and Methods. Electron micrographs were digitally recorded from the BSE signal.

Statistical analysis and image processing

Statistical significance for experimental data was analyzed using Student's two-tailed *t*-test. *P* values were set at a cutoff of 1% and are represented by asterisks in the graphs, as described in the legends. Sample size was >5, and at least three biological replicates were used for all measurements. Images were processed with Adobe Photoshop and GIMP (www.gimp.org), analyzed with ImageJ and assembled with Inkscape (inkscape.org). The integrated map of the binary interaction network was generated with Cytoscape (Shannon et al., 2003). Further details can be found in the supplementary Materials and Methods.

Yeast two hybrid (Y2H) and network analysis

Y2H screens were performed as described previously (Dreze et al., 2010). Briefly, open reading frames (ORFs) encoding fragments of CLUB/AtTRS130 (C1-C3) and TRS120 (T1, T2, T3) were transferred by Gateway cloning into the GAL4 DNA-binding domain (DB) encoding he Y2H vector pDEST-pPC97, and subsequently transformed into the yeast strain Y8930. These constructs were screened by yeast mating against a collection of 12,000 *Arabidopsis* ORFs fused to the Gal4 activation domain (AD) in the yeast strain Y8800 (Weßling et al., 2014). Screening was carried out as a binary mini-pool screen, i.e. each DB-ORF was screened against pools of 188 AD-ORFs. Interactions were assayed by growth on selective plates using the HIS3 reporter, and using 1 mM 3-amino-1,2,4-triazole (3-AT) to suppress background growth. This primary screen was carried out once and interaction candidates were identified by Sanger sequencing. All candidate interactions were verified by pairwise one-on-one mating in three independent experiments. Only pairs scoring positives in all three assays were considered as bona fide interaction partners.

Communities in the *Arabidopsis* protein-protein interactome network are groups of proteins more highly connected to each other than to the rest of the network; they are defined based on enrichment in functionally consistent gene ontology annotations (Arabidopsis Interactome Mapping Consortium, 2011). Communities were detected by an edge-based algorithm and presented using an 'Edge-weighted Spring Embedded Layout' algorithm.

Acknowledgements

We thank Prof. Grill and members of the Botany department for their support. A special thanks to Prof. Torres-Ruiz for sharing his expertise and lending support for the embryo analyses. We are exceedingly grateful to Andreas Czempiel for technical assistance. Thanks to Miriam Abele for a critical appraisal of the text. We thank the Advanced Light Microscopy Facility (ALMF) at the European Molecular Biology Laboratory (EMBL) and Abberior Instruments for support. Aliaksandr Halavatyi (ALMF, EMBL Heidelberg) helped with image processing and colocalization analysis. Silvia Dobler in the laboratory of Andreas Klingl (LMU) prepared samples for electron microscopy. David Ehrhardt, Karin Schumacher, Glenn Hicks, NASC and the RIKEN Bioresource Center shared published or public resources.

Competing interests

The authors declare no competing or financial interests.

Author contributions

Conceptualization: R.R., N.K., D.G., A.S., S.A., K.R., H.E., F.S., F.F.A.; Methodology: R.R., N.K., D.G., A.S., M.A., S.A., K.R., H.E., F.S., M.L., E.F., G.W., P.F.-B., F.F.A.; Software: R.R., N.K., A.S., S.A., P.F.-B.; Validation: R.R., N.K., A.S., K.R., H.E., F.S., E.F., G.W., P.F.-B., F.F.A.; Formal analysis: R.R., N.K., D.G., A.S., M.A., S.A., K.R., H.E., F.S., M.L., P.F.-B., F.F.A.; Investigation: R.R., N.K., D.G., A.S., M.A., S.A., K.R., H.E., F.S., M.L., F.F.A.; Resources: M.A., M.L., G.W., P.F.-B., R.P.B., F.F.A.; Data curation: R.R., N.K., F.F.A.; Writing - original draft: F.F.A.; Writing - review & editing: R.R., N.K., D.G., A.S., S.A., M.L., P.F.-B., R.P.B., F.F.A.; Visualization: F.F.A.; Supervision: P.F.-B., F.F.A.; Project administration: F.F.A.; Funding acquisition: F.F.A.

Funding

This work was supported by Deutsche Forschungsgemeinschaft grant DFG AS110/4-7 to F.F.A., by Deutsche Forschungsgemeinschaft grant SFB 924/2-A10 to P.F-B. and by grant 2012-0050 from the Knut och Alice Wallenbergs Stiftelse (Shapesystems) to R.P.B.

Data availability

Sequence data used in this article can be found in the *Arabidopsis* Genome Initiative database (www.arabidopsis.org) under the following accession numbers: ECHIDNA, At1g09330; CLUB, At5g54440; TRS120, At5g11040. Further accession numbers for markers, polymorphsisms and TRAPPII subunits are listed in Tables S1 to S4. All data that support the conclusions of this study are available from the corresponding author upon request.

Supplementary information

Supplementary information available online at http://dev.biologists.org/lookup/doi/10.1242/dev.169201.supplemental

References

Arabidopsis Interactome Mapping Consortium (2011). Evidence for network evolution in an arabidopsis interactome map. *Science* **333**, 601-607.

Barr, F. A. (2013). Rab GTPases and membrane identity: causal or inconsequential? *J. Cell Biol.* **202**, 191-199.

Bolte, S. and Cordelières, F. P. (2006). A guided tour into subcellular colocalisation analysis in light microscopy. *J. Microsc.* **224**, 213-232.

Boutté, Y., Jonsson, K., McFarlane, H. E., Johnson, E., Gendre, D., Swarup, R., Friml, J., Samuels, L., Robert, S. and Bhalerao, R. P. (2013). ECHIDNA-mediated post-Golgi trafficking of auxin carriers for differential cell elongation. *Proc. Natl. Acad. Sci. USA* **110**, 16259-16264.

Chow, C.-M., Neto, H., Foucart, C. and Moore, I. (2008). Rab-A2 and Rab-A3 GTPases define a trans-golgi endosomal membrane domain in Arabidopsis that contributes substantially to the cell plate. *Plant Cell* **20**, 101-123.

Collins, N. C., Thordal-Christensen, H., Lipka, V., Bau, S., Kombrink, E., Qiu, J.-L., Hückelhoven, R., Steins, M., Freialdenhoven, A., Somerville, S. C. et al. (2003). SNARE-protein-mediated disease resistance at the plant cell wall. *Nature* **425**, 973-977.

Costes, S. V., Daelemans, D., Cho, E. H., Dobbin, Z., Pavlakis, G. and Lockett, S. (2004). Automatic and quantitative measurement of protein-protein colocalization in live cells. *Biophys. J.* **86**, 3993-4003.

Dettmer, J., Hong-Hermesdorf, A., Stierhof, Y.-D. and Schumacher, K. (2006). Vacuolar H+-ATPase activity is required for endocytic and secretory trafficking in arabidopsis. *Plant Cell Online* **18**, 715-730.

Drakakaki, G., van de Ven, W., Pan, S., Miao, Y., Wang, J., Keinath, N. F., Weatherly, B., Jiang, L., Schumacher, K., Hicks, G. et al. (2012). Isolation and proteomic analysis of the SYP61 compartment reveal its role in exocytic trafficking in Arabidopsis. *Cell Res.* **22**, 413-424.

Dreze, M., Monachello, D., Lurin, C., Cusick, M. E., Hill, D. E., Vidal, M. and Braun, P. (2010). *High-Quality Binary Interactome Mapping*, 2nd edn. Elsevier Inc.

Fan, X., Yang, C., Klisch, D., Ferguson, A., Bhaellero, R. P., Niu, X. and Wilson, Z. A. (2014). ECHIDNA protein impacts on male fertility in arabidopsis by mediating trans-golgi network secretory trafficking during anther and pollen development. *Plant Physiol.* **164**, 1338-1349.

Fendrych, M., Synek, L., Pečenková, T., Toupalová, H., Cole, R., Drdová, E., Nebesářová, J., Šedinová, M., Hála, M., Fowler, J. E. et al. (2010). The *Arabidopsis* exocyst complex is involved in cytokinesis and cell plate maturation. *Plant Cell* **22**, 3053-3065.

Fujiwara, M., Uemura, T., Ebine, K., Nishimori, Y., Ueda, T., Nakano, A., Sato, M. H. and Fukao, Y. (2014). Interactomics of Qa-SNARE in arabidopsis thaliana. *Plant Cell Physiol.* **55**, 781-789.

Gendre, D., Oh, J., Boutté, Y., Best, J. G., Samuels, L., Nilsson, R., Uemura, T., Marchant, A., Bennett, M. J., Grebe, M. et al. (2011). Conserved Arabidopsis ECHIDNA protein mediates trans-Golgi-network trafficking and cell elongation. *Proc. Natl. Acad. Sci. USA* **108**, 8048-8053.

Gendre, D., McFarlane, H. E., Johnson, E., Mouille, G., Sjodin, A., Oh, J., Levesque-Tremblay, G., Watanabe, Y., Samuels, L. and Bhalerao, R. P. (2013). Trans-golgi network localized ECHIDNA/Ypt interacting protein complex is required for the secretion of cell wall polysaccharides in arabidopsis. *Plant Cell* **25**, 2633-2646.

Gendre, D., Jonsson, K., Boutté, Y. and Bhalerao, R. P. (2015). Journey to the cell surface—the central role of the trans-Golgi network in plants. *Protoplasma* **252**, 385-398.

Groen, A. J., Sancho-Andrés, G., Breckels, L. M., Gatto, L., Aniento, F. and Lilley, K. S. (2014). Identification of trans-Golgi network proteins in Arabidopsis thaliana root tissue. *J. Proteome Res.* **13**, 763-776.

Ito, E., Ebine, K., Choi, S., Ichinose, S., Uemura, T., Nakano, A. and Ueda, T. (2018). Integration of two RAB5 groups during endosomal transport in plants. *Elife* **7**, e34064.

Jaber, E., Thiele, K., Kindzierski, V., Loderer, C., Rybak, K., Jürgens, G., Mayer, U., Söllner, R., Wanner, G. and Assaad, F. F. (2010). A putative TRAPPII tethering factor is required for cell plate assembly during cytokinesis in Arabidopsis. *New Phytol.* **187**, 751-763.

Jonsson, K., Boutté, Y., Singh, R. K., Gendre, D. and Bhalerao, R. P. (2017). Ethylene regulates differential growth via BIG ARF-GEF-dependent post-golgi secretory trafficking in arabidopsis. *Plant Cell* **29**, 1039-1052.

Kang, B.-H., Nielsen, E., Preuss, M. L., Mastronarde, D. and Staehelin, L. A. (2011). Electron tomography of RabA4b- and PI-4Kβ1-labeled trans golgi network compartments in arabidopsis. *Traffic* **12**, 313-329.

Kim, J. J., Lipatova, Z. and Segev, N. (2016). TRAPP complexes in secretion and autophagy. *Front. Cell Dev. Biol.* **4**, 20.

Kirchhelle, C., Chow, C.-M., Foucart, C., Neto, H., Stierhof, Y.-D., Kalde, M., Walton, C., Fricker, M., Smith, R. S., Jérusalem, A. et al. (2016). The specification of geometric edges by a plant Rab gtpase is an essential cell-patterning principle during organogenesis in arabidopsis. *Dev. Cell* **36**, 386-400.

Kosetsu, K., Matsunaga, S., Nakagami, H., Colcombet, J., Sasabe, M., Soyano, T., Takahashi, Y., Hirt, H. and Machida, Y. (2010). The MAP kinase MPK4 is required for cytokinesis in arabidopsis thaliana. *Plant Cell Online* **22**, 3778-3790.

Li, R., Rodriguez-Furlan, C., Wang, J., van de Ven, W., Gao, T., Raikhel, N. V. and Hicks, G. R. (2017). Different endomembrane trafficking pathways establish apical and basal polarities. *Plant Cell* **29**, 90-108.

Matthes, M. and Torres-Ruiz, R. A. (2016). Boronic acid treatment phenocopies *monopteros* by affecting PIN1 membrane stability and polar auxin transport in *Arabidopsis thaliana* embryos. *Development* **143**, 4053-4062.

McFarlane, H. E., Watanabe, Y., Gendre, D., Carruthers, K., Levesque-Tremblay, G., Haughn, G. W., Bhalerao, R. P. and Samuels, L. (2013). Cell wall polysaccharides are mislocalized to the vacuole in echidna Mutants. *Plant Cell Physiol.* **54**, 1867-1880.

Nguema-Ona, E., Vicré-Gibouin, M., Gotté, M., Plancot, B., Lerouge, P., Bardor, M. and Driouich, A. (2014). Cell wall O-glycoproteins and N-glycoproteins: aspects of biosynthesis and function. *Front. Plant Sci.* **5**, 1-12.

Pérez-Pérez, J. M., Candela, H. and Micol, J. L. (2009). Understanding synergy in genetic interactions. *Trends Genet.* **25**, 368-376.

Qi, X. and Zheng, H. (2011). Arabidopsis TRAPPII is functionally linked to Rab-A, but not Rab-D in polar protein trafficking in *trans* -Golgi network. *Plant Signal. Behav.* **6**, 1679-1683.

Qi, X., Kaneda, M., Chen, J., Geitmann, A. and Zheng, H. (2011). A specific role for Arabidopsis TRAPPII in post-Golgi trafficking that is crucial for cytokinesis and cell polarity. *Plant J.* **68**, 234-248.

Ravikumar, R., Steiner, A. and Assaad, F. F. (2017). Multisubunit tethering complexes in higher plants. *Curr. Opin. Plant Biol.* **40**, 97-105.

Robert, S., Chary, S. N., Drakakaki, G., Li, S., Yang, Z., Raikhel, N. V. and Hicks, G. R. (2008). Endosidin1 defines a compartment involved in endocytosis of the brassinosteroid receptor BRI1 and the auxin transporters PIN2 and AUX1. *Proc. Natl. Acad. Sci. USA* **105**, 8464-8469.

Rosquete, M. R., Davis, D. J. and Drakakaki, G. (2018). The plant trans-golgi network: not just a matter of distinction. *Plant Physiol.* **176**, 187-198.

Rutherford, S. and Moore, I. (2002). The Arabidopsis Rab GTPase family: another enigma variation. *Curr. Opin. Plant Biol.* **5**, 518-528.

Rybak, K., Steiner, A., Synek, L., Klaeger, S., Kulich, I., Facher, E., Wanner, G., Kuster, B., Zarsky, V., Persson, S. et al. (2014). Plant cytokinesis is orchestrated by the sequential action of the TRAPPII and exocyst tethering complexes. *Dev. Cell* **29**, 607-620.

Sanderfoot, A. A., Assaad, F. F. and Raikhel, N. V. (2000). The Arabidopsis genome. an abundance of soluble N-ethylmaleimide-sensitive factor adaptor protein receptors. *Plant Physiol.* **124**, 1558-1569.

Sasabe, M., Boudolf, V., De Veylder, L., Inze, D., Genschik, P. and Machida, Y. (2011a). Phosphorylation of a mitotic kinesin-like protein and a MAPKKK by cyclin-dependent kinases (CDKs) is involved in the transition to cytokinesis in plants. *Proc. Natl. Acad. Sci. USA* **108**, 17844-17849.

Sasabe, M., Kosetsu, K., Hidaka, M., Murase, A. and Machida, Y. (2011b). Arabidopsis thaliana MAP65-1 and MAP65-2 function redundantly with MAP65-3/PLEIADE in cytokinesis downstream of MPK4. *Plant Signal. Behav.* **6**, 743-747.

Shannon, P., Markiel, A., Owen, O., Baliga, N. S., Wang, J. T., Ramage, D., Amin, N., Schwikowski, B. and Ideker, T. (2003). Cytoscape: a software environment for integrated models of biomolecular interaction networks. *Genome Res.* **13**, 2498-2504.

Smertenko, A., Assaad, F., Baluška, F., Bezanilla, M., Buschmann, H., Drakakaki, G., Hauser, M.-T., Janson, M., Mineyuki, Y., Moore, I. et al. (2017). Plant cytokinesis: terminology for structures and processes. *Trends Cell Biol.* **27**, 885-894.

Staehelin, L. A. and Kang, B.-H. (2008). Nanoscale architecture of endoplasmic reticulum export sites and of golgi membranes as determined by electron tomography. *Plant Physiol.* **147**, 1454-1468.

Steiner, A., Rybak, K., Altmann, M., McFarlane, H. E., Klaeger, S., Nguyen, N., Facher, E., Ivakov, A., Wanner, G., Kuster, B. et al. (2016a). Cell cycle-regulated PLEIADE/AtMAP65-3 links membrane and microtubule dynamics during plant cytokinesis. *Plant J.* **88**, 531-541.

Steiner, A., Müller, L., Rybak, K., Vodermaier, V., Facher, E., Thellmann, M., Ravikumar, R., Wanner, G., Hauser, M.-T. and Assaad, F. F. (2016b). The membrane-associated Sec1/Munc18 KEULE is required for phragmoplast microtubule reorganization during cytokinesis in arabidopsis. *Mol. Plant* **9**, 528-540.

Swarbreck, D., Wilks, C., Lamesch, P., Berardini, T. Z., Garcia-Hernandez, M., Foerster, H., Li, D., Meyer, T., Muller, R., Ploetz, L. et al. (2008). The arabidopsis information resource (TAIR): gene structure and function annotation. *Nucleic Acids Res.* **36**, 1009-1014.

Thellmann, M., Rybak, K., Thiele, K., Wanner, G. and Assaad, F. F. (2010). Tethering factors required for cytokinesis in arabidopsis. *Plant Physiol.* **154**, 720-732.

Uemura, T. and Nakano, A. (2013). Plant TGNs: dynamics and physiological functions. *Histochem. Cell Biol.* **140**, 341-345.

Vernoud, V., Horton, A. C., Yang, Z. and Nielsen, E. (2003). Analysis of the small GTPase gene superfamily of arabidopsis. *Plant Physiol.* **131**, 1191-1208.

Weßling, R., Epple, P., Altmann, S., He, Y., Yang, L., Henz, S. R., McDonald, N., Wiley, K., Bader, K. C., Gläßer, C. et al. (2014). Convergent targeting of a common host protein-network by pathogen effectors from three kingdoms of life. *Cell Host Microbe* **16**, 364-375.

Yang, X. (1998). Specific binding to a novel and essential Golgi membrane protein (Yip1p) functionally links the transport GTPases Ypt1p and Ypt31p. *EMBO J.* **17**, 4954-4963.